# Rheometric investigation on the temporal shear thickening of dilute micellar solutions of $C_{14}$-, $C_{16}$-, and $C_{18}$TAB/NaSal

Jalal Dehmoune,[a] Jean Paul Decruppe, Olivier Greffier, and Hong Xu

*Laboratoire de Physique des Milieux Denses, Equipe des Fluides Complexes, Université Paul Verlaine Metz, I.P.E.M. 1 Bd. F. Arago 57078 Metz, France*

(Received 30 May 2007; final revision received 7 October 2007)

**Synopsis**

The rheological behavior and especially the rheopexy phenomena of dilute self-assembled solutions in the presence of a counterion are examined in stationary and transient shear flows. In the first part, a continuous and gradually increasing strain is applied on the same sample. We study the effect of the initial shear rate, the temporal variation of the viscosity, and the hysterisis between charge and discharge curves. The results show that the properties of shear thickening are independent of the initial shear rate. In the second part, fresh samples are successively subjected to increasing shear strains; this method allows us to follow the evolution of the rheological characteristics during long measuring durations and gives us a distinct picture of the behavior per shear rate. In both cases, we confirm that the chain length has a strong influence on the emergence and amplitude of the shear thickening. It was also found by studying the start-up flow behavior that the structure at equilibrium is composed of bigger structures for longer chain lengths. The maximum of the viscosity in the shear thickening transition occurs in a range of lower shear rates when enough time is given to the system to undertake the formation of the shear induced structure. Considering this result, we introduce the concept of "temporal shear thickening transition."
 [DOI: 10.1122/1.2933352]

## I. INTRODUCTION

The dissolution of amphiphilic surfactant molecules in an aqueous solvent can give several structures such as cylindrical [Kalus *et al.* (1982)] or spherical micelles [Bendedouch *et al.* (1983)]. This arrangement is the result of the particular structure of the surfactant molecule which is built with two antagonist parts: A hydrophilic polar head and a hydrophobic aliphatic chain. The micelles formation process is obtained when the critical micellar concentration (CMC) is exceeded. These dilute systems are considered as complex fluids; they are characterized by different structural transitions depending on several parameters, for example: concentration, counterion, co-surfactant, temperature,…; but the transition which retains our attention is the one driven by the hydrodynamic field. Indeed it has been shown that the increase of the shear rate or of the shear stress up to a critical value causes a shear thickening transition in dilute micellar solutions [Rehage and Hoffmann (1982); Rehage *et al.* (1986); Wunderlich *et al.* (1987); Hu *et al.*

[a]Author to whom correspondence should be addressed; electronic mail: dehmoune@univ-metz.fr

(1994); Liu and Pine (1996); Hu *et al.* (1998a, b); Gamez-Corrales *et al.* (1999)]. It is widely admitted that the shear thickening is caused by the building up of shear induced structures (SIS) [Rehage and Hoffmann (1982); Rehage *et al.* (1986); Wunderlich *et al.* (1987); Rehage and Hoffmann (1988); Hoffmann *et al.* (1991); Hu *et al.* (1994); Liu and Pine (1996); Boltenhagen *et al.* (1997a); Boltenhagen *et al.* (1997b); Hu *et al.* (1998a, b); Gamez-Corrales *et al.* (1999); Dehmoune *et al.* (2007)] also called shear induced phases. In spite of many efforts given for 30 years, many aspects of the increase of the viscosity (rheopexy) are not yet fully understood. The organization of the micelles in the SIS under flow is different from the arrangement at equilibrium; however in previous works, divergences still remain on the formation mechanism and the constitution of the SIS [Rehage and Hoffmann (1982); Rehage *et al.* (1986); Wunderlich *et al.* (1987); Liu and Pine (1996); Boltenhagen *et al.* (1997a); Escalante and Hoffmann (2000)].

Part of the answer may be revealed by the transient mode flow. Effectively the temporal flow can be a source of remarkable information about the shear thickening transition. This approach was used by different authors on several surfactant systems in the dilute domain [Rehage and Hoffmann (1988); Liu and Pine (1996); Hu *et al.* (1998a, b); Gamez-Corrales *et al.* (1999)]. Previous works gave many different values of the induction time ($T_{ind}$) which is the time necessary for the transition to occur; it varies from a few to thousands of seconds depending on the systems and on the applied strain [Rehage and Hoffmann (1982); Escalante and Hoffmann (2000); Bandyopadhyay *et al.* (2000); Bandyopadhyay and Sood (2001)]. The variation of shear stress (or viscosity) as function of time up to a constant value for a constant shear rate is apparently the signature of the coexistence between SIS and a fluid phase [Hu *et al.* (1998a, b); Liu and Pine (1996); Hoffmann *et al.* (1991)]. Other characteristics are the irregular fluctuations of the shear stress which appear in the shear thickening domain, it should accompany the highly instable flow resulting from the SIS formation [Hu *et al.* (1998b); Berret *et al.* (2000)]. Another interesting property concerns the time relaxation of the shear stress which informs us about the disintegration process of the SIS toward the equilibrium phase [Hu *et al.* (1994); Hu *et al.* (1998a); Escalante and Hoffmann (2000)].

The hysterisis characterizes the reversibility of the rheological behavior as a function of the shear rate at short measuring time. This flow mode was studied on micellar shear thickening systems [Escalante and Hoffmann (2000); Bandyopadhyay and Sood (2001)].

Many aspects of the transient behavior of the dilute micellar solutions are still not yet understood because of the few existing experimental studies and the complexity of the behavior exhibited by the micellar systems. The present work tries to shed some light on the transient behavior of shear thickening systems. In our investigation, three surfactants were chosen in the family $C_nTAB$ where the molecules have the same polar head but different chain length built with 14, 16, and 18 carbon molecules. The steady state behavior of these micellar solutions was well described in a previous paper [Boltenhagen *et al.* (1997a)], in which one shows that the chain length plays an important part in the micellar formation. The concentration conditions being the same, a longer chain length will give a longer micellar structure which will be more easily oriented in the flow. The chain length has a strong macroscopic effect on the rheological response of the studied systems [Boltenhagen *et al.* (1997a)]. This result reveals that the comparison between different surfactant systems is in fact quite complicated. In order to contribute to the understanding of the shear thickening transition, this paper presents a detailed study of the stationary and transient behavior of dilute micellar systems. Our approach consists of the study of the behavior, at first under continuous applied shear rates and in a second part where each strain is applied to a fresh and unshared sample. In addition this study takes into account the surfactant chain length as the main variable parameter.

The paper is organized as follows: Sec. II describes the samples and apparatus; Sec. III gives our rheometric results, and in Sec. IV we present the conclusions.

## II. SAMPLE AND APPARATUS

The systems used in this work are ionic surfactants and they are commercially available: the myristyltrimethylammonium bromide ($C_{14}$TAB) was obtained from Acros organics. The cetyltrimethylammonium bromide ($C_{16}$TAB), the octadecyltrimethylammonium bromide ($C_{18}$TAB) and the organic counterion sodium salicylate (NaSal) were purchased from Aldrich.

The products are dissolved in distilled water without any further purification. The concentration of the surfactant/counterion mixture is 3 mM/3 mM. For the ($C_n$TAB) series studied in this work, we have checked in the literature that a concentration of 3 mM is slightly above the critical micellar concentration (CMC) even in the presence of the counterion [Hartmann (1997); Basu Ray *et al.* (2005)]. The CMC is the concentration corresponding to the formation of micelles. The surfactant fraction and the solvent volume are prepared by carefully weighing the required amount with a precision of $\pm 10^{-4}$ g. The ratio of the concentration between the surfactants and the counterion is kept to unity. This will provide an optimal growth of the micelles [Liu and Pine (1996)] and a maximum strength of the shear thickening [Hu *et al.* (1994); Hartmann (1997)].

For the rheometric measurements, we have used a shear rate controlled rheometer (RFS III, TA Instruments) fitted with a Couette cell, the dimensions of which are 34 mm for the outer diameter, 32 mm for the inner one, thus leading to a 1 mm gap. All the experiments were carried out in a Couette cell; this geometry is the best adapted to the study of the flow of low concentrations solutions. The temperature is kept constant within $23 \pm 0.3$ °C by a circulating bath of water and a lid is added to prevent evaporation. Due to the low viscosity of the solutions, the stress produced in the flow is small and each flow curve was repeated several times in order to be sure of the consistency of our results.

The sample is submitted to shearing when we loaded in the Couette cell; this is why each experience is started after the 600 s to permit the relaxation of the sample before the beginning of the measurements.

## III. RHEOMETRY RESULTS

### A. Continuous mode flow

We define the "continuous mode flow" as the experiments which consist in subjecting the same sample to a range of shear rates varying gradually from low values to higher ones or inversely. We have applied six shear rate per decade and each shear rate during 600 s. In this kind of nonstop shear flow, the outcoming rheological results transmitted by $C_n$TAB solutions allow us to detect the historical shear effect on shear thickening properties.

#### *1. Continuous steady flow: Initial shear rate effect*

In this section we study the effect of the initial shear rate ($\dot{\gamma}_{ini}$) on the global steady state behavior and principally on the emergence and the aspect of the shear thickening. The application of different ($\dot{\gamma}_{ini}$)'s on a same system can inform us about the historic solicitation effect on the properties of the shear thickening.

In Fig. 1, we give typical rheological curves, $\eta$ vs. $\dot{\gamma}$ obtained in the stationary mode flow. We applied continuous but progressively increasing shear rates during a measuring time of 600 s for each point as in Dehmoune *et al.* (2007). For the three systems, different

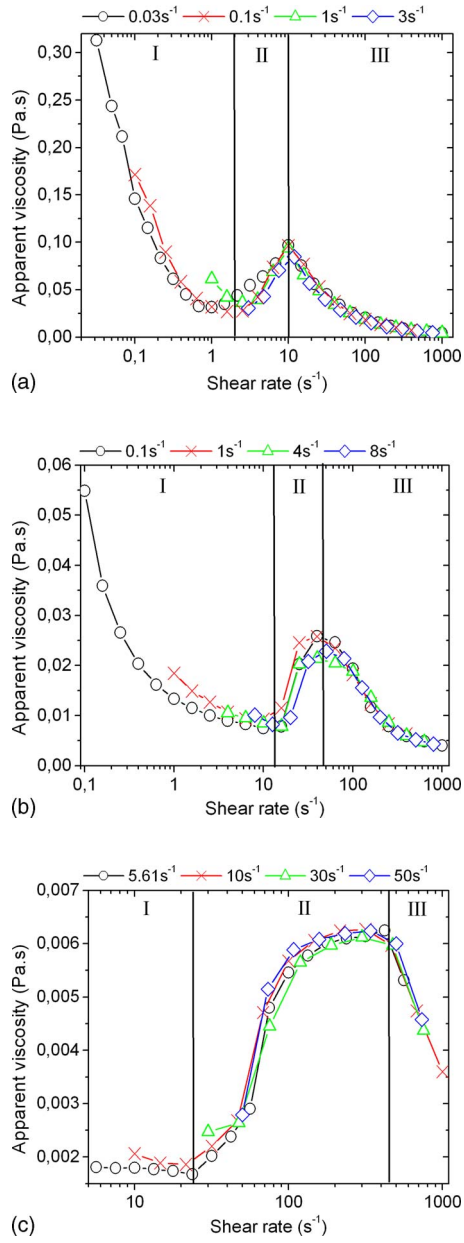


**FIG. 1.** Effect of the initial shear rate ($\dot{\gamma}_{ini}$) in the steady state flow under controlled strain of the solutions at 3 mM/3 mM: (a) $C_{18}$TAB/NaSal, (b) $C_{16}$TAB/NaSal, and (c) $C_{14}$TAB/NaSal.

flow curves were obtained, each set of data comes from a fresh sample and corresponds to a given initial shear rate. These results also show the chain length influence (Fig. 1).

In a previous work [Dehmoune *et al.* (2007)], we have characterized the stationary behavior of the systems investigated in this work; it allows us to choose the initial shear rate values which precede the shear thickening transition. For $C_{18}$TAB, we have started the steady shear flow at initial shear rates ($\dot{\gamma}_{ini}$) of 0.03, 0.1, 1, and 3 $s^{-1}$ [see Fig. 1(a)];

for $C_{16}$TAB the $\dot{\gamma}_{ini}$'s were 0.1, 1, 4, and 8 $s^{-1}$ [see Fig. 1(b)] and finally we chose to apply the following shear rates 5.61, 10, 30, and 50 $s^{-1}$ as $\dot{\gamma}_{ini}$ for the $C_{14}$TAB system [see Fig. 1(c)].

The curves of Fig. 1 confirm the existence of three regimes delimited by shear rates as described in Boltenhagen *et al.* (1997b) and Gamez-Corrales *et al.* (1999). The descriptions of the different regimes which characterize the flow of the shear thickening solutions are: *Regime I* (Newtonian or shear thinning) which precedes the shear thickening transition. *Regime II* represents the interval where the shear thickening transition appears. *Regime III* (shear thinning) occurs after reaching a maximum of the viscosity $\eta_{max}$. The critical shear rate $\dot{\gamma}_c$ is defined as the value where the shear thickening transition occurs.

Figure 1(a) displays the results for $C_{18}$TAB. The flow curves of different initial shear rates $\dot{\gamma}_{ini}$ exhibit the same evolution; the shear thickening amplitude does not change and the critical shear rate ($\dot{\gamma}_c$) remains close to 2.0 $s^{-1}$. The same observation is obtained for the other systems $C_{16}$TAB and $C_{14}$TAB [see Figs. 1(b) and 1(c)].

### 2. Continuous transient flow

The operating mode is the same as in Sec. III A 1, where a new sample is subjected to the progressive and continuous action of the shearing flow. Here, for the same shear rate as in Sec. III A 1, the variations of the stress are recorded as a function of time during 600 s. The main question arising from these experiments resumes to: How does the temporal viscosity of the sample behave in the three regimes and especially close to the critical shear rate $\dot{\gamma}_c$?

In Fig. 2 we have recorded temporal viscosity values for each shear rate for the three shear thickening systems. We have also reproduced the results of the continuous steady flow behavior of Fig. 1 to facilitate the comparison between the two recordings. These results confirm that the shear thickening occurs at the same critical shear rate ($\dot{\gamma}_c$) (see Fig. 2).

We observe an overshoot at the inception of the flow except for $C_{14}$TAB [Fig. 2(c)]. This suggests that there is little deformation and micelle alignment under shear rate during the initial induction [Hu *et al.* (1993a)]. The overshoot is more pronounced when the chain length is longer. It should be pointed out that, for solutions of longer chain lengths, the recording of a higher overshoot is a sign of a bigger structure or of entanglements. In addition we observe a remarkable behavior; irregular fluctuations of the viscosity around a medium value begin to appear at the critical shear rate ($\dot{\gamma}_c$).

It is worth noticing that the rheological behavior in gradual transient and steady flows is in agreement (see Fig. 2). The gradual transient mode allows having a detailed view of the temporal behavior of the fluid sample subjected to the different shearing rates. In this way, periodical fluctuations of the viscosity in the shear thickening domain have been revealed.

### 3. Hysterisis effect

Another experimental investigation in the continuous flow mode was also carried out. We have looked for a possible hysterisis effect and compared its sensitivity to short and long measuring times. This kind of investigation is lacking for dilute surfactants solutions. In Fig. 3, we display flow curves ($\eta$ vs. $\dot{\gamma}$) for the $C_n$TAB/NaSal systems. We performed "charge" and "discharge" flows under controlled shear rate with a measuring time of 10 s and 600 s per point. The charge flow consists of subjecting the sample to progressive and continuous shear rates from low values to higher ones. In the discharge flow, $\dot{\gamma}$ decreases continuously from high to low values. Notice that the discharge curve

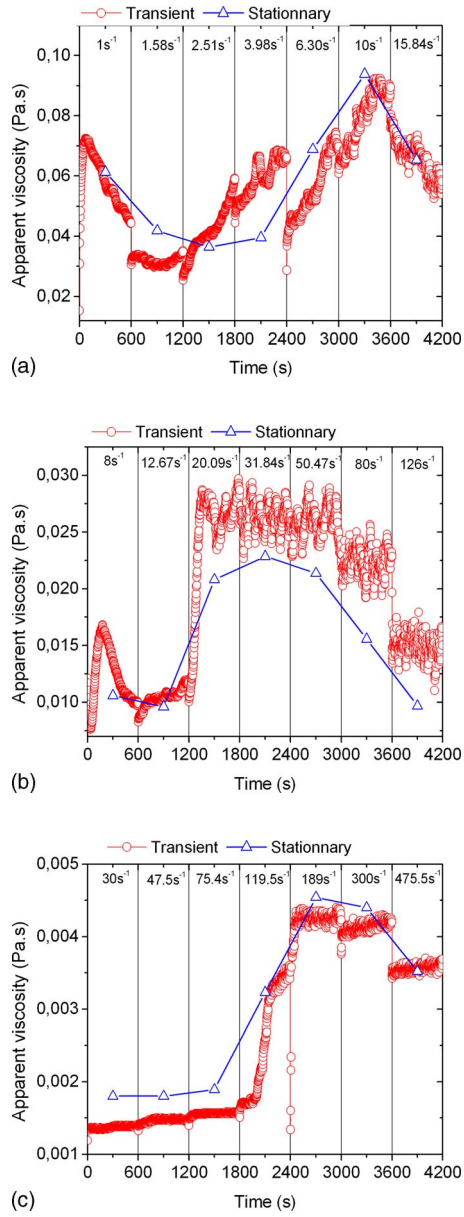


**FIG. 2.** Viscosity variation in continuous transient and stationary mode flows under controlled strain of the systems: (a) $C_{18}$TAB/NaSal, (b) $C_{16}$TAB/NaSal, and (c) $C_{14}$TAB/NaSal.

is obtained immediately after the end of the charge flow. It is expected that the charge and discharge curves would be notably different if the scanning time is too short. It is also interesting to study the hysterisis as function of the chain length.

As we can see in Fig. 3, all the systems present qualitatively the same evolution. Curves obtained with a measuring time of 10 s per point have a shear thickening amplitude smaller than the one obtained with 600 s per point. We think that the proportion of the SIS is higher for a given shear rate when the measuring duration is longer. For our systems the two curves only superimpose at high shear rates, we suppose that we are in

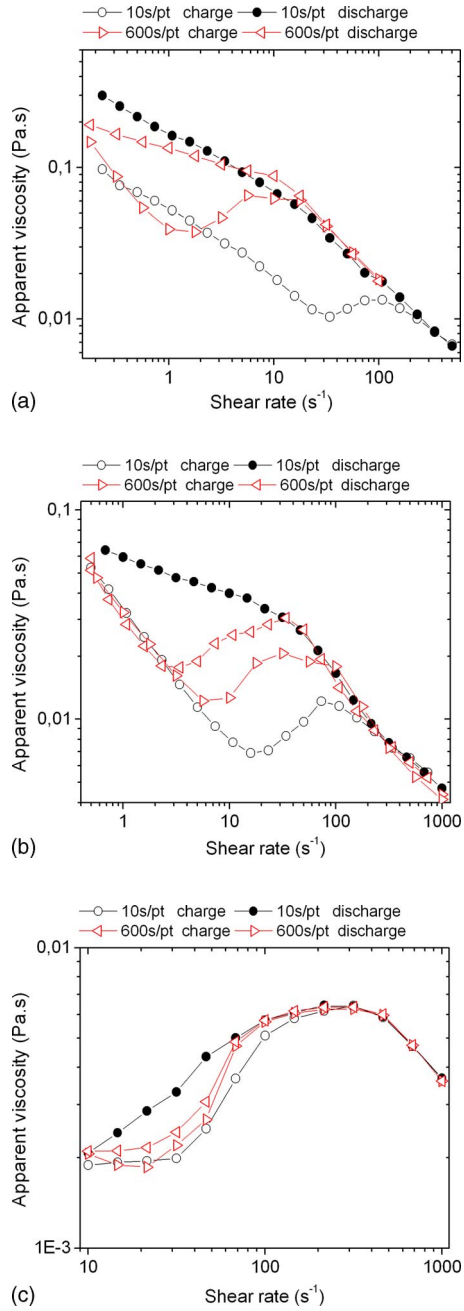


**FIG. 3.** Hysterisis effect in the curves $\eta(\dot{\gamma})$ for the following systems: (a) $C_{18}$TAB/NaSal, (b) $C_{16}$TAB/NaSal, and (c) $C_{14}$TAB/NaSal.

the presence of a single phase (no phase coexistence). Furthermore, in regime III, the flow behavior (after shear thickening) is independent of the chain length as mentioned in our previous publication [Dehmoune *et al.* (2007)]. It was already established that it is independent of the concentration, the chain length, the mode flow (stress or strain controlled).

At low shear rates, the charge curves show $\eta$ values smaller than the ones observed in the discharge, except for $C_{14}$TAB where they almost superimpose. The difference is more pronounced at low strain because in the charge curve there is not enough energy given to the micelles orientation process. On the other hand, the discharge process is related to the microscopic relaxation of the SIS. These curves indicate that the SIS formation and disintegration processes need more time than the 600 s per point to be achieved. A direct correlation can be observed between the chain length and the area between the charge and discharge curves: The shorter the chain, the smaller this area (see Fig. 3). We can relate the large difference between the charge and discharge curves (hysterisis) to a probable coexistence between the SIS and a fluid phase which has a lower viscosity; this question will be quantitavely discussed in the following sections.

## B. Discontinuous mode flow

A new investigation method was used here in shear flows of dilute micellar solutions. We call it "discontinuous mode flow"; in this experimental procedure, a single new sample is used for each value of the shear rate. For the three systems of this study, each point of the viscosity curve corresponds to a fresh sample. All the samples of a same solution came from the same mother solution. The sample is not presheared and has never been presheared before the experiment. This procedure allows showing the shape of the growth mechanism of the shear induced structure (SIS) which should depend on shear rate.

In the discontinuous measurements, it is possible to follow the shear viscosity variations as a function of time over a long measuring period; we record the behavior evolution over 10 800 s (3 h) under a given shear rate. This protocol is more adapted to the study of the solutions behavior at higher measuring time. Two physical reasons led us to choose the measuring time; on the one hand, it should be long enough to follow the evolution of the sample in a domain which has never been studied before; on the other hand, it should be short enough to prevent evaporation. Taking into account these limitations, we adopted a measuring time of 10 800 s.

### *1. Discontinuous transient mode flow*

The discontinuous transient rheological investigation is adapted to show the temporal evolution of $\eta$ at a given shear rate value $\dot{\gamma}$. Therefore we will extend our experiments to a large interval of shear rates which covers the different flow regimes. We summarize in Figs. 4, 5, and 6 typical transient viscosity curves $\eta$ $(t)$ for $C_{18}$TAB, $C_{16}$TAB, and $C_{14}$TAB systems, respectively.

The important parameter is the induction time ($T_{\text{ind}}$); it corresponds to the time interval between the beginning of the measurement of the recorded parameter which can be either the shear stress or the viscosity and the moment when it reaches a constant value under the applied shear rate. Previous experiences in transient mode flow have reported a large difference in the $T_{\text{ind}}$ values [Rehage and Hoffmann (1982); Wunderlich *et al.* (1987); Rehage and Hoffmann (1988); Hoffmann *et al.* (1991); Hu *et al.* (1994); Berret (1997); Swanson-Vethamuthu *et al.* (1998); Escalante and Hoffmann (2000); Bandyopadhyay *et al.* (2000); Basu Ray *et al.* (2005)].

In Fig. 4, the viscosity variation curves of $C_{18}$TAB at $\dot{\gamma}$ equal to 0.5 and 1 $s^{-1}$ show first a sharp peak of the viscosity at very short times. After the first peak, the viscosity increases slowly during 10 800 s without reaching any constant value. In consequence no steady state is obtained for these strains but the final measured value is close to the viscosity maximum $\eta_{\max}$=200 mPa s obtained in the steady state mode [see Fig. 1(a)]. It

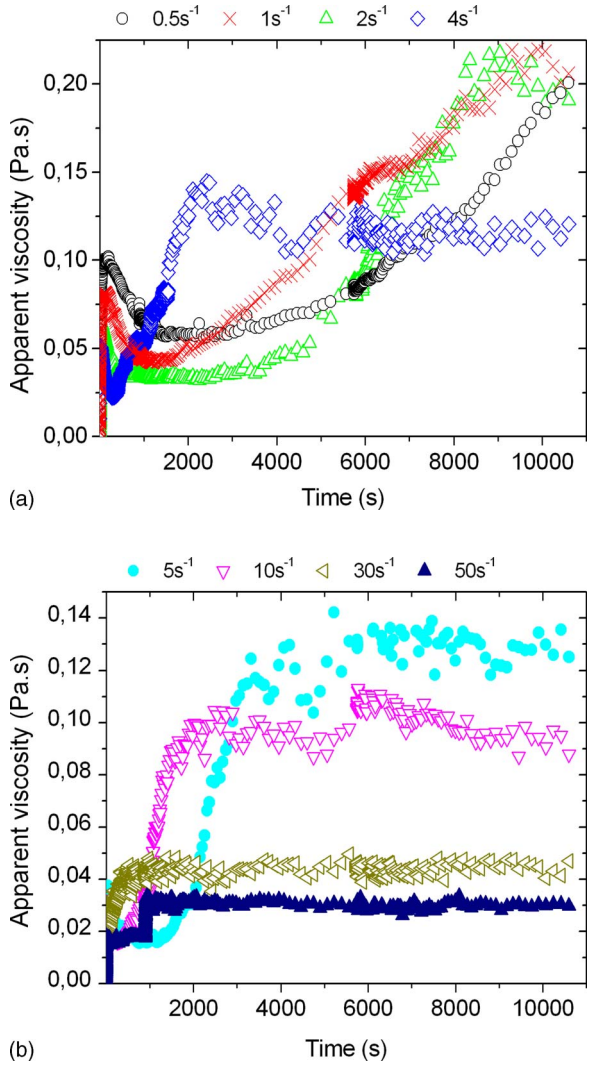


**FIG. 4.** Time evolution of the apparent viscosity $\eta$ for different shear rate $\dot{\gamma}$ for $C_{18}$TAB/NaSal: (a) low shear rates and (b) high shear rates.

can be assumed that this maximum value corresponds to the complete formation of the SIS. The shear rate values of 0.5 and 1 $s^{-1}$ are smaller than the critical value which is close to 2.6 $s^{-1}$. This suggests that one can apply a weak shearing during a sufficient period in order to bring enough energy to trigger the shear thickening transition and reach the maximum viscosity value.

Near the critical shear rate $\dot{\gamma}$ of 2 $s^{-1}$ a plateau of the viscosity is obtained after an induction time ($T_{ind}$) of about 8000 s.

The computed viscosity is also approximatively 200 mPa s, which is larger than the maximum $\eta_{max}$=150 mPa s recorded in the steady flow at 600 s/pt [see Fig. 1(a)]. Obtaining the viscosity maximum allows us to think that the SIS fills a large part of the gap in the discontinuous shear flow.

At intermediate shear rates of 4, 5, and 10 $s^{-1}$ [see Figs. 4(a) and 4(b)] the increase of

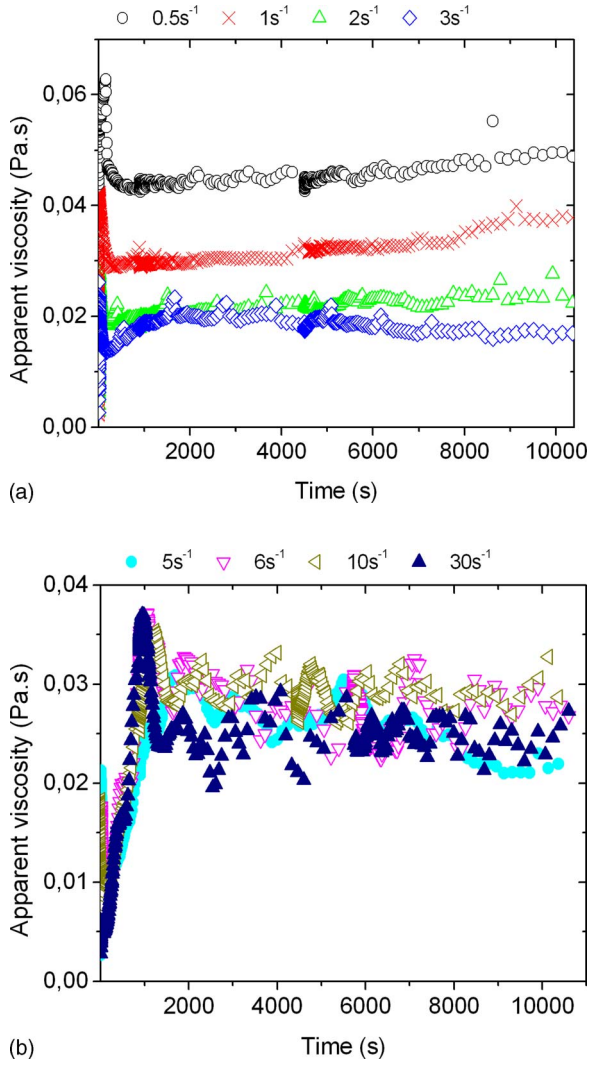


**FIG. 5.** Time evolution of the apparent viscosity $\eta$ for different shear rate $\dot{\gamma}$ for $C_{16}$TAB/NaSal: (a) low shear rates and (b) high shear rates.

the viscosity occurs after an induction time ($T_{ind}$) of about 1800 s. It is important to notice that, for these three values, the final value of the viscosity is close to $\eta_{max}$ [see Fig. 1(a)] and its mean value is 120 mPa s.

For the higher shear rates of 30 and 50 $s^{-1}$ [see Fig. 4(b)], the induction time is sharply reduced to a few seconds. The viscosities corresponding to 30 and 50 $s^{-1}$ are, respectively, 30 and 40 mPa s. It should be the zone corresponding to the shear thinning in Fig. 1(a).

In Figs. 5(a) and 5(b) we carefully studied the time variation of the apparent viscosity in a wide range of shear rates of $C_{16}$TAB. Figure 5(a) shows the viscosity evolution at lower shear rates: 0.5, 1, 2, and 3 $s^{-1}$. These measurements provide convincing evidence that the increase of $\dot{\gamma}$ will lead to a decrease of $\eta$. This region corresponds to the shear thinning regime before the shear thickening transition.

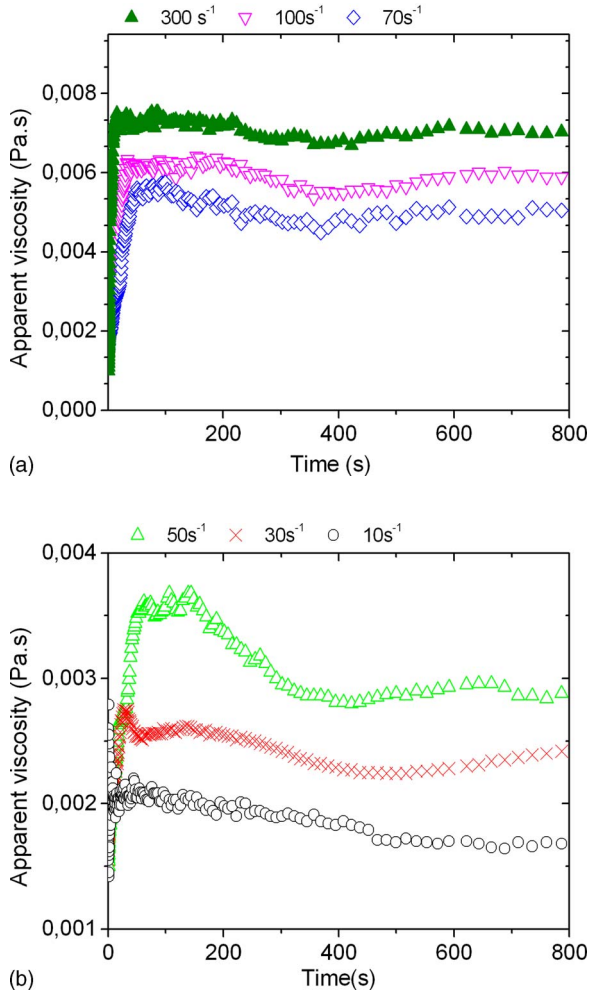


**FIG. 6.** Time evolution of the apparent viscosity $\eta$ for different shear rate $\dot{\gamma}$ for $C_{14}$TAB/NaSal: (a) low shear rates and (b) high shear rates.

Thereafter, all the curves corresponding to $\dot{\gamma}$ values of 5, 6, 10, and 30 $s^{-1}$ [Fig. 5(b)] show qualitatively the same evolution: the apparent viscosity $\eta$ increasing up to three times the initial viscosity (before shear thickening transition) during an induction time $T_{ind}$ of 2000 s. It is shown that the viscosity plateau has the same value of about 28 mPa s and corresponds to the maximum of the viscosity $\eta_{max}$ recorded in Fig. 1(b) which characterizes the shear thickening of $C_{16}$TAB at discontinuous steady shear flows.

The behavior of $C_{14}$TAB was also studied in transient rheometry. The curves of the apparent viscosity $\eta$ vs. time $t$ under controlled shear rates are plotted in Figs. 6(a) and 6(b). For this system, the viscosity $\eta$ quickly stabilizes to a constant value after induction times which are small compared to $C_{16}$TAB and $C_{18}$TAB and never exceeding 200 s. The stationary viscosity values correspond to the one obtained in steady state [see Fig. 1(c)].

We also found the emergence of irregular viscosity fluctuations in the transient flow behavior in the shear thickening region of $C_{16}$TAB and $C_{18}$TAB solutions. This phenom-

enon is widely observed [Hu *et al.* (1996); Berret *et al.* (1995); Bandyopadhyay and Sood (2001)]. It could be an unstable flow and not a rheological artifact of the measurement. No significant fluctuations were observed for $C_{14}$TAB.

As in Sec. III A 2 in the stationary mode flow (see Figs. 1 and 4–6), each system is characterized by a given maximum amplitude in the shear thickening which corresponds to a viscosity $\eta_{max}$. This maximum is probably related to the filling of the entire or part of the gap by the SIS. In the transient mode flow, we have found that the viscosity maximum $\eta_{max}$ value is identitical for continuous and discontinuous shear flows for $C_{16}$TAB and $C_{14}$TAB but not for $C_{18}$TAB. For the last system, the maximum viscosity $\eta_{max}$ could be reached in continuous mode (Fig. 1) only if $\dot{\gamma}$ is kept close to the critical shear rate $\dot{\gamma}_c$ ($4.5\ s^{-1} < \dot{\gamma} < 10\ s^{-1}$) and if the shear flow is applied for a long enough duration (>1800 s). This is why we consider that the steady state curve at 600 s per point only represents a certain state of the system. Thus we confirm the results of Rehage *et al.* (1986) who observed that the shape of the steady state curves changes with the measuring time. This feature can be easily seen in the transient flows where the time evolution of $\eta$ is more complicated. The kinetics of the shear thickening transition is characterized by a large induction time $T_{ind}$ for the lower shear rates. The difference in the induction times $T_{ind}$ are due to the quantity of energy brought by the shear flow. The increase of $\eta$ up to the saturation value is faster when the shear rates are higher or when the shearing duration is longer. We shall call this shear thickening phenomenon which depends on the combination of time and shear rate "temporal shear thickening."

### *2. Overshoot in the discontinuous transient mode flow*

Figure 7 represents a zoom of Figs. 4–6 where an overshoot is observed in the curves $\eta(t)$ as mentioned in Berret (1997). This phenomenon can be seen in the enlargement of the viscosity curve $\eta(t)$ at the inception of the flow and during the induction period.

It is shown that the behavior at the inception of the flow for $C_{18}$TAB and $C_{16}$TAB is similar and presents four distinct regions (see Fig. 7). The first region consists of a rather rapid increase of $\eta$ for a few seconds. After this short period of shearing, the viscosity of the fluid reaches the maximum viscosity. One can notice that this value is more pronounced when $\dot{\gamma}$ is smaller and is obtained after a duration time ranging from a few seconds to a maximum of 100 s (see Fig. 7) strongly depending on $\dot{\gamma}$. In this first response of the samples, the viscosity maximum is certainly due to the elastic response of the sample which opposes the disentanglement action of the flow. This resistance leads to higher values of $\eta$ at lower shear rates after longer times. For example, in the case of $C_{18}$TAB [see Fig. 7(a)], for $\dot{\gamma}=0.5\ s^{-1}$, $\eta_{max}$ is approximately 11 mPa s and it is reached in 100 s; on the contrary at $\dot{\gamma}=30\ s^{-1}$, the viscosity maximum equals 4 mPa s and is reached in 1 s.

Notice that for all the systems we did not present time evolution of the apparent viscosity at higher shear rate because they reach a constant shear stress value rapidly (few seconds).

It was established that the overshoot on the short time scale is located in the shear thinning regime [Berret *et al.* (2000)]; we also think that this character certainly results from the entanglement.

Qualitatively the same evolution is observed for the viscosity of $C_{16}$TAB; it reaches a maximum value and this first part can have a duration of a few seconds [see Fig. 7(b)]. At this stage the fluids response is dominated by the elastic character. The process of micelles disentanglement is faster with higher shear rates, because the energy brought by the flow is more important.

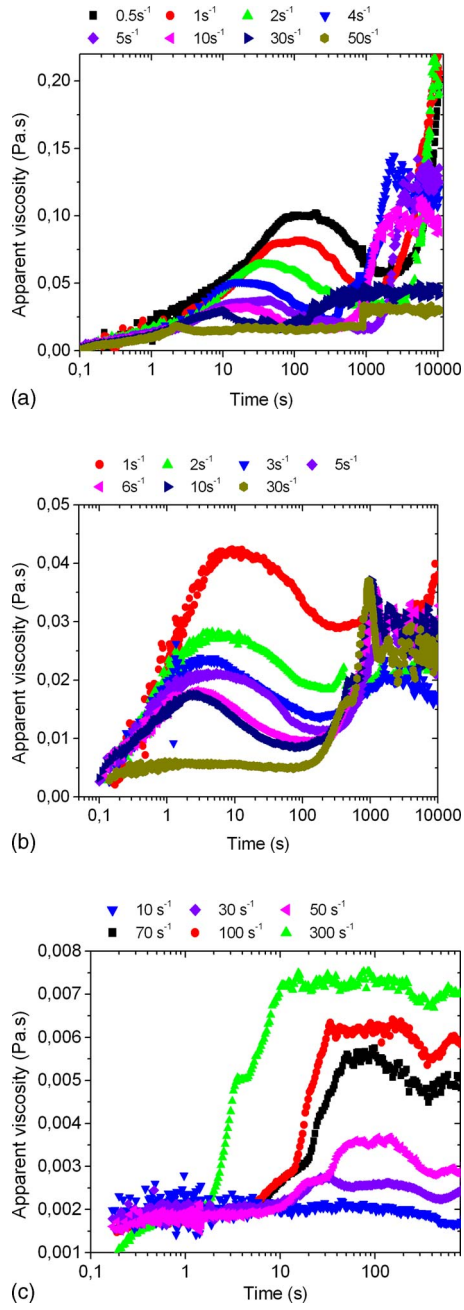


**FIG. 7.** Enlargement of the transient viscosity $\eta$ at the inception of the flow concerning: (a) $C_{18}$TAB/NaSal, (b) $C_{16}$TAB/NaSal, and (c) $C_{14}$TAB/NaSal.

In the second region of $\eta(t)$, the viscosity tends to decrease slowly with time. A decrease of the viscosity is observed before it reaches the maximum value, because the entanglements are broken under the shear flow effect. The third region of $\eta(t)$ consists of another increase of the viscosity, but this one is due to the SIS formation when the system undergoes a phase transition which we term temporal shear thickening (see Sec. III B 1).

The fourth region is due to the shear thickening transition, where collisions between the micelles are at the origin of the growth of the SIS and consequently of the viscosity. A progressive growth is visible at different shear rates for $C_{18}$TAB and $C_{16}$TAB but not for $C_{14}$TAB. This shows that the temporal shear thickening depends on the chain length.

One can notice that the overshoot is not observed for $C_{14}$TAB [Fig. 7(c)] which means that this behavior depends on the chain length. It informs us about the structure at equilibrium. The absence of overshoot for $C_{14}$TAB leads to the hypothesis that at equilibrium no entanglement or network structure exists in this system. On the other hand, the overshoot is more pronounced for $C_{18}$TAB than for $C_{16}$TAB. This suggests that the longer chain length of $C_{18}$TAB makes the formation of a network of micelles at equilibrium easier in comparison to $C_{16}$TAB at the same concentration.

### *3. Stress relaxation*

For our systems, stress relaxation experiments have also been performed in the following way: We submitted systems $C_{18}$TAB and $C_{16}$TAB to shear rates of, respectively, 4 and 6 $s^{-1}$ during 10 800 s. We choose these shear values in the way to obtain the maximum viscosity ($\eta_{max}$) SIS and reach probably the complete formation of the SIS. After subjecting the samples to constant shear flow, the motion of the rotor is suddenly stopped and the stress variations are recorded as a function of the time $t$. The study of the stress relaxation can give information on the disintegration process of the SIS towards the equilibrium phase. It is known that the shear induced structures have much longer relaxation times than those of the equilibrium phase [Hu *et al.* (1993b)].

In Figs. 8(a), 8(b), and 8(c) we report the stress relaxation $\tau(t)$ of $C_{18}$TAB, $C_{16}$TAB, and $C_{14}$TAB as well as the theoretical adjustment of the experimental points by a double exponential decay function [Hu *et al.* (1994)]. This adjustment was not possible on $C_{14}$TAB; it confirms that no micelles entanglement is present in this system

$$\tau = A_1 e^{(-t/T1)} + A_2 e^{(-t/T2)},$$

where $T_1$ and $T_2$ are the two relaxation times, $A_1$ and $A_2$ the amplitude of the two individual functions. The quantitative values resulting from the fitting process are gathered in Table I.

Generally speaking, the fitting parameters ($T_i$ and $A_i$) are found to be larger for $C_{18}$TAB, the surfactant with the longer aliphatic chain; for each member of the family, $C_{16}$TAB or $C_{18}$TAB, the $T_i$'s are of the same order of magnitude indicating that the two relaxation processes are of nearly equal importance although they do not happen over the same time interval ($T_1 \ll T_2$ for both surfactants).

The first relaxation time, $T_1$, is found to be nearly the same for $C_{16}$TAB and $C_{18}$TAB, respectively, 19.9 and 20.12 s; when the flow is suddenly stopped, the stress in both samples relaxes nearly in the same way; the physical process responsible for the stress decay is the same in both samples; we can reasonably assume that during the first stage the orientating action of the flow will rapidly decrease leading to a disorientation of individual micelles (not engaged in the SIS) and of the SIS; once this process is achieved, the SIS can disintegrate with a relaxation time $T_2$ nearly twice as long for $C_{18}$TAB than for $C_{16}$TAB; this result is in favor of the assumption according to which the aliphatic chain length of the surfactant molecule is an important factor in the formation and the structure of the SIS.

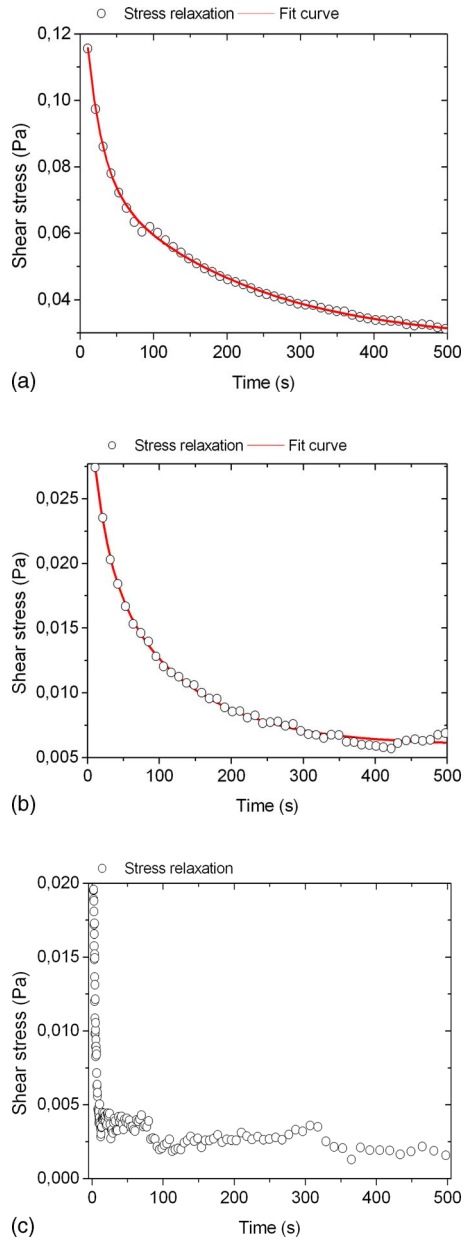


**FIG. 8.** Shear stress relaxation vs. time of: (a) $C_{18}$TAB/NaSal and (b) $C_{16}$TAB/NaSal.

**TABLE I.** Fit parameters of stress relaxation curves.

| Parameter | $T_1$ | $T_2$ | $A_1$ | $A_2$ |
|---|---|---|---|---|
| $C_{16}$TAB | 19,9 | 114 | 0,012 | 0,015 |
| $C_{18}$TAB | 20,12 | 201 | 0,065 | 0,052 |

## IV. CONCLUSION

In this experimental work, rheometric measurements were performed in order to study the shear thickening behavior of aqueous micellar solutions of $C_n$TAB/NaSal at the low concentration of 3 mM/3 mM.

In a first part, we have developed measurements with continuous and progressive shear flows. We investigated stationary as well as transient continuous flows, and have examined the hysterisis on our systems. The results are significant because they show that there is no influence of the historical solicitation of the shear rate on the properties of the shear thickening. Continuous temporal shear flows is an original view on the flow behavior of the shear thickening systems; overshoots are observed at the inception of the flow and viscosity fluctuations appear at the critical shear rate. The reversibility of the global behavior is more pronounced for small chain lengths. Our results confirm the coexistence of the SIS and of a fluid phase in the shear thickening transition.

In a second part, discontinuous shear flows were performed and each shear rate corresponds to a fresh sample. The maximal amplitude of the shear thickening is related to a viscosity maximum $\eta_{max}$ at a particular shear rate. This saturation value is close to the viscosity maximum in the shear thickening region in the steady state of each system $C_n$TAB. We have observed in the discontinuous transient flow of $C_{16}$TAB and $C_{18}$TAB that $\eta_{max}$ is reached at shear rates much lower than $\dot{\gamma}_c$ but after a much longer shearing time, the surfactants systems acquiring sufficient energy which is the combination of the shear rate and the flow duration. Furthermore, our systems show an induction period $T_{ind}$ which varies from one system to another and which depends on the shear rate.

In the rheometric transient response, we also found oscillations of the viscosity; the most pronounced oscillations are recorded when the maximum of the viscosity is reached and for longer chain length. No viscosity oscillations were observed for $C_{14}$TAB.

The mechanical response in start-up experiments of discontinuous shear flows is also remarkable. It informs about the structure at the equilibrium; the amplitude of the overshoot confirms that the structure is entangled and is formed by aggregates bigger when the chain length is longer.

The energy given by the shear rate causes microstructural changes, a continuous kinetic coagulation process where small micelles are converted into supramolecular structures. The friction between these bigger structures is assumed to be at the origin of the rheopexy of micellar solutions [Rehage and Hoffmann (1988)]. These elements and data confirm the important role played by the chain length in the macroscopic behavior; the shear thickening changes drastically with the chain length and structural changes are at the origin of the increase of the viscosity.

We also established that the shear thickening is triggered by a combination of the shear rate intensity and the shearing duration. We found that the longer the shearing duration, the lower the value of the shear rate needed to start the shear thickening. Thus, one can ask if a critical shear rate $\dot{\gamma}_c$ at all exists in these low concentration surfactant solutions. These results also emphasized the fact that only very little energy is needed to change the isotropic organization of the micelles in the sample at equilibrium to give a fluid with completely different rheophysical properties.

$C_{14}$TAB behaves in a way different from $C_{16}$TAB and $C_{18}$TAB; the $C_{14}$TAB system presents no overshoot, no viscosity fluctuations, and the relaxation is very fast. These experimental results confirm that we are at a frontier in the rheophysical behavior when the aliphatic chain length of the micelles is the physical parameter of the study.

## References


Bandyopadhyay, R., G. Basappa, and A. K. Sood, "Observation of chaotic dynamics in dilute sheared aqueous solutions of CTAT," Phys. Rev. Lett. **84**, 2022 (2000).

Bandyopadhyay, R., and A. K. Sood, "Chaotic dynamics in shear-thickening surfactant solutions," Europhys. Lett. **56**, 447 (2001).

Basu Ray, G., I. Chakraborty, S. Ghosh, S. P. Moulik, and R. Palepu, "Self-aggregation of alkyltrimethylammonium bromides (C[10]-, C[12]-, C[14]-, and C[16]TAB) and their binary mixtures in aqueous medium: A critical and comprehensive assessment of interfacial behavior and bulk properties with reference to two types of micelle formation," Langmuir **21**, 10958 (2005).

Bendedouch, D., S. H. Chen, and W. C. Koehler, "Determination of interparticle structure factors in ionic micellar solutions by small angle neutron scattering," J. Phys. Chem. **87**, 2621 (1983).

Berret, J. F., "Transient rheology of wormlike micelles," Langmuir **13**, 2227 (1997).

Berret, J. F., R. Gamez-Corrales, S. Lerouge, and J. P. Decruppe, "Shear-thickening transition in surfactant solutions: New experimental features from rheology and flow birefringence," Eur. Phys. J. E **2**, 343 (2000).

Boltenhagen, P., Y. T. Hu, E. Matthys, and D. J. Pine, "Inhomogeneous structure formation and shear-thickening in worm-like micellar solutions," Europhys. Lett. **38**, 389 (1997a).

Boltenhagen, P., Y. T. Hu, E. Matthys, and D. J. Pine, "Observation of bulk phase separation and coexistence in a sheared micellar solution," Phys. Rev. Lett. **79**, 2359 (1997b).

Dehmoune, J., J. P. Decruppe, O. Greffier, and H. Xu, "Rheometric and rheo-optical investigation on the effect of the aliphatic chain length of the surfactant on the shear thickening of dilute worm-like micellar solutions," Rheol. Acta published online (2007).

Escalante, J., and H. Hoffmann, "Non-linear rheology and flow-induced transition of a lamellar-vesicle phase in ternary systems of alkyldimethyl oxide/alcohol/water," Rheol. Acta **39**, 309 (2000).

Gamez-Corrales, R., J. F. Berret, L. M. Walker, and J. Oberdisse, "Shear thickening in dilute solutions of wormlike micelles," Langmuir **15**, 6755 (1999).

Hartmann, V., "Experimental study of shear thickening and shear induced transitions for micellar solutions," Ph.D. thesis, University of Metz (1997).

Hoffmann, S., A. Rauscher, and H. Hoffmann, "Shear induced micellar structures," Ber. Bunsenges. Phys. Chem. **95**, 153 (1991).

Hu, Y., C. V. Rajaram, S. Q. Wang, and A. M. Jamieson, "Shear thickening behavior of a rheopectic micellar solution: Salt effects," Langmuir **10**, 80 (1994).

Hu, Y. T., P. Boltenhagen, E. Matthys, and D. J. Pine, "Shear thickening in low-concentration solutions of wormlike micelles. I. Direct visualization of transient behavior and phase transitions," J. Rheol. **42**, 1185 (1998a); Hu, Y. T., P. Boltenhagen, E. Matthys, and D. J. Pine, "Shear thickening in low-concentration solutions of wormlike micelles. II. Slip, fracture, and stability of the shear-induced phase," J. Rheol. **42**, 1209 (1998b).

Hu, Y., S. Q. Wang, and A. M. Jamieson, "Rheological and flow birefringence studies of a shear thickening complex fluid-A surfactant model system," J. Rheol. **37**, 531 (1993a).

Hu, Y., S. Q. Wang, and A. M. Jamieson, "Kinetic studies of a shear thickening micellar solution," J. Colloid Interface Sci. **156**, 31 (1993b).

Kalus, J., H. Hofmann, K. Reizlein, W. Ulbricht, and K. Ibel Ber, "Small angle neutron scattering measurements on ionic detergent solutions with rodlike micelles," Ber. Bunsenges. Phys. Chem. **86**, 31 (1982).

Liu, C. H., and D. J. Pine, "Shear-induced gelation and fracture in micellar solutions," Phys. Rev. Lett. **77**, 2121 (1996).

Rehage, H., I. Wunderlich, and H. Hoffmann, "Shear-induced phase transitions in dilute aqueous surfactant solutions." Prog. Colloid Polym. Sci. **72**, 51 (1986).

Rehage, H., and H. Hoffmann, "Rheological properties of viscoelastic surfactant systems," J. Phys. Chem. **92**, 4712 (1988).

Rehage, H., and H. Hoffmann, "Shear induced phase transitions in highly dilute aqueous detergent solutions," Rheol. Acta **21**, 561 (1982).

Swanson-Vethamuthu, M., E. Feitosa, and W. Brown, "Salt-induced sphere-to-disk transition of octadecyltrimethylammonium bromide micelles," Langmuir **14**, 1590 (1998).

Wunderlich, I., H. Hoffmann, and H. Rehage, "Flow birefringence and rheological measurements on shear induced micellar structures," Rheol. Acta **26**, 532 (1987).